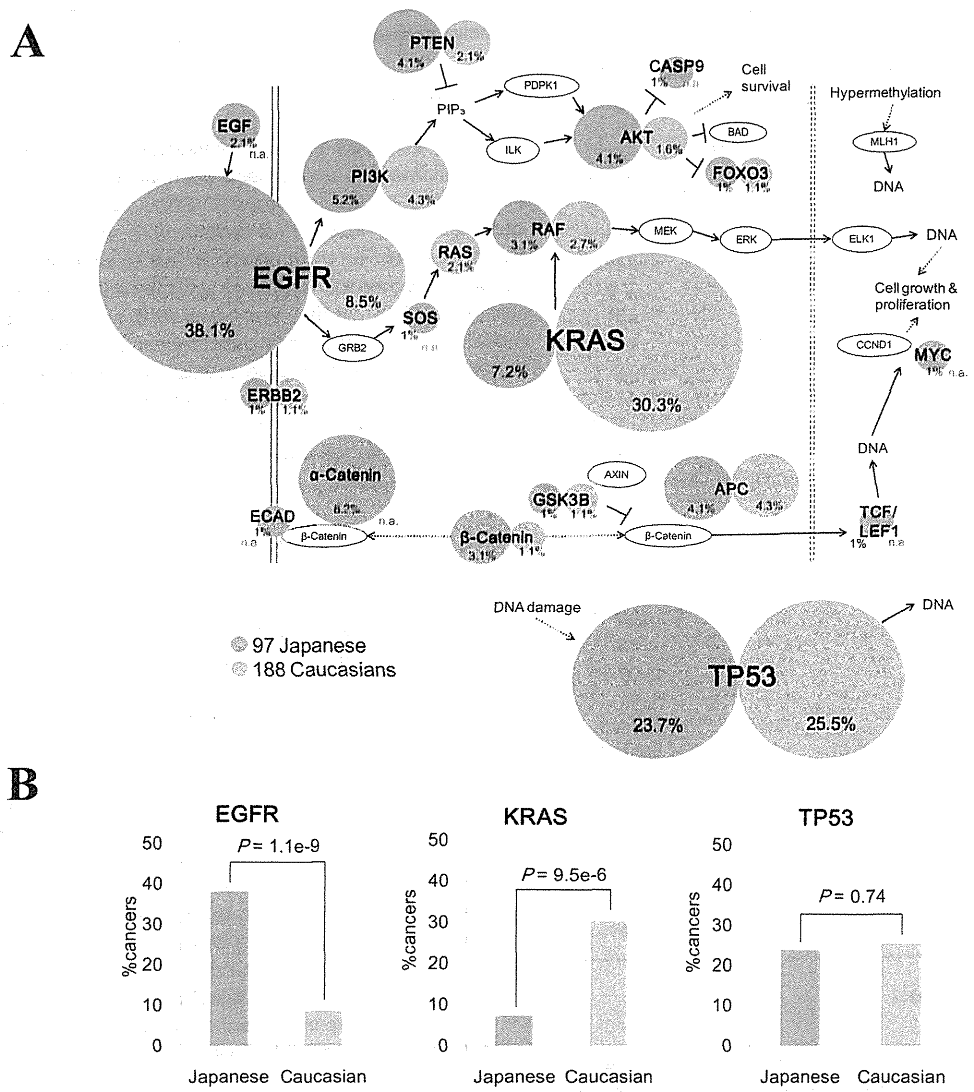

Fig. 2

Figure 2. The EGFR/Ras pathways in Japanese and Caucasian populations. (**A**) Mutation patterns in the endometrial cancer pathway that was detected in the enrichment analysis are shown. The size of the circle represents the population of the cancers harboring the SNVs in the corresponding gene (percentage is also shown in the margin). SNVs in this study and the external dataset in Caucasian populations are shown in red and blue circles, respectively. n.a.: mutation frequencies were not available. (**B**) Comparison of mutation ratio of EGFR, KRAS and TP53 genes among both datasets. The p-values were calculated by two-sample test for equality of proportions.

doi: 10.1371/journal.pone.0073484.g002

sequencing of cancer tissues and their normal tissue counterparts (Figure S12 in File **S1**).

Identification of highly mutated genes

We detected genes which were significantly enriched with SNVs by calculating the expected number of cancers with SNVs in the gene. The length of total CDS regions was represented in N (approximately 30.8 M bases). When one patient harbored total of m SNVs, the probability that the patient harbors SNVs in the gene t (length: n) was calculated as P:

$$P_{m,t,n} = 1 - \left(1 - \frac{m}{N}\right)^n$$

The sum of P in 97 cancers was represented in the expected number of cancers with SNVs in the gene t. The p-values of the

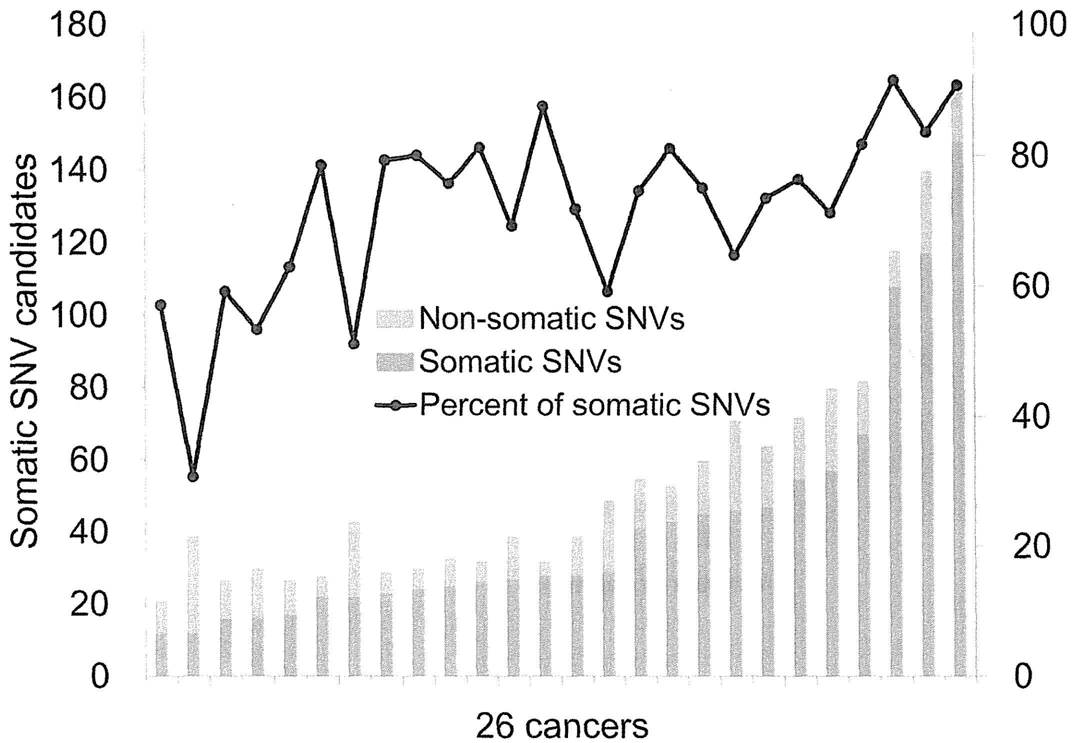

Fig. 3

Figure 3. Fidelity of the germline SNV detection in cancer exome analysis. Somatic SNV candidates were identified by using 26 cancer exomes and each normal counterpart. Correct somatic SNVs and false positives were shown in pink and blue bars, respectively. The 26 cancers used for the analysis were sorted by the increasing total number of SNVs (x-axis).
doi: 10.1371/journal.pone.0073484.g003

observed number were calculated by the Poisson probability function using R ppois.

Statistical approach to enrichment analyses

To examine the enrichment of mutations in functional protein domains, we mapped the SNVs to domains using InterProScan [52] and assigned them to the Catalogue of Somatic Mutations in Cancer (COSMIC). We analyzed the enrichment of the SNVs in the same domains as the mutations that were provided by the COSMIC. The p-values for the observed mutations in these domains were calculated using their hypergeometric distributions (R phyper). Briefly, the domains in which the SNVs were enriched statistically significantly than the expected number of SNVs in the given length of the domain were selected. For estimating the expected number, the total number of the SNVs belonging to the gene was divided by the gene length. For this analysis, we used genes harboring five or more SNVs in the coding region and three or more SNVs in the domain.

We assigned SNVs to pathways as described by the Kyoto Encyclopedia of Genes and Genomes (KEGG) and calculated the enrichments of the SNVs in the pathways. The mutation rate *M* represented the ratio of the average number of mutated genes to the total number of genes (17,175) that were used in our study. The expected value for the number of cancers with SNVs in pathway *t* was designated λ and calculated from the mutation rate *M* and the number of genes in the pathway *n* as follows:

$$\lambda_{t,n}=\left\{1-(1-M)^n\right\}\times 97$$

The p-value for the observed number of cancers with SNVs in pathway *t* was calculated by the Poisson probability function using R ppois.

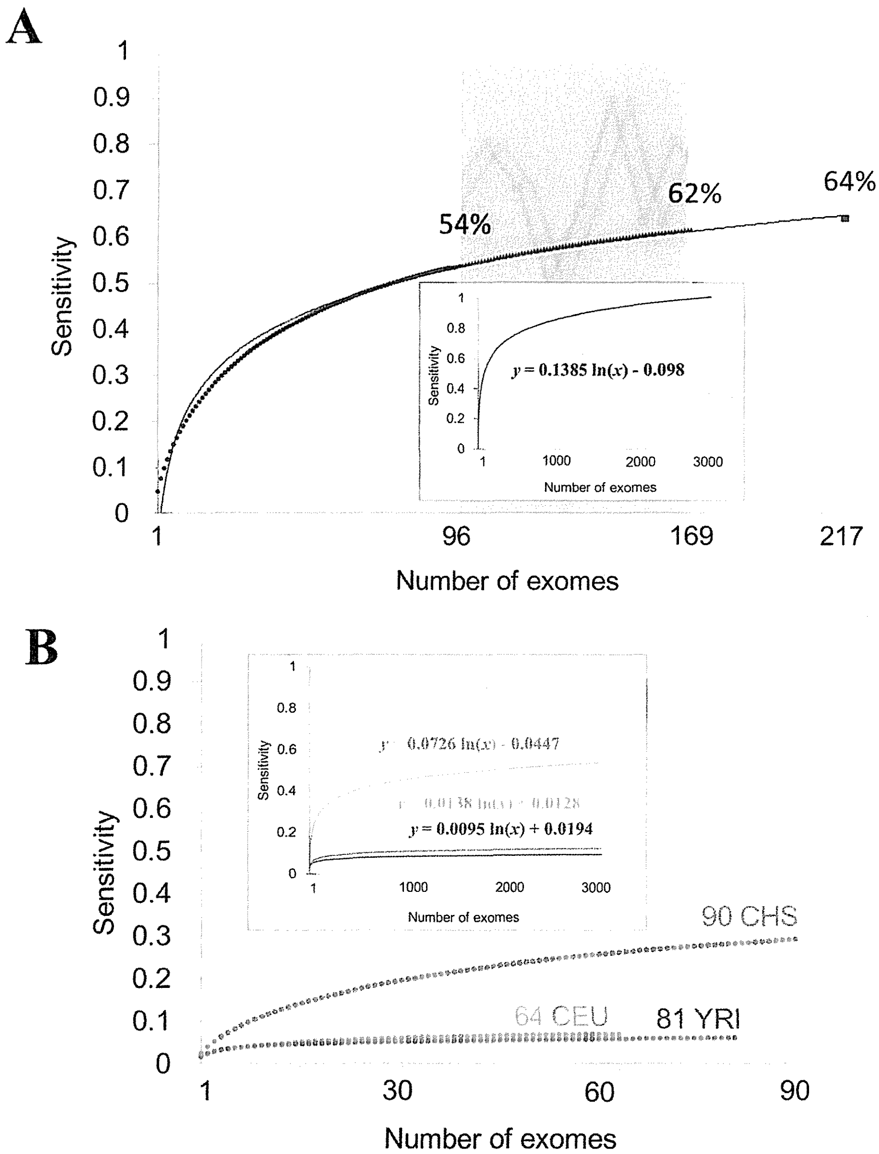

Fig. 4

Figure 4. Discriminative powers of detecting germline SNVs using external references. (**A**) The power of detecting germline SNVs considering mutual overlap between other Japanese individuals. Sensitivity represents the proportion of germline SNVs correctly detected. The datasets used to exclude the germline SNVs are shown on the x axis. The inset represents the extrapolation of the graph. Fitting curve of the graph is also shown. (**B**) Discriminative powers of three different ethnic groups for the germline SNVs in 97 Japanese cancers. Sensitivities for detecting germline SNVs are shown by the following colors; green: Chinese; purple: Yoruba; orange: Caucasian.

doi: 10.1371/journal.pone.0073484.g004

Estimate of discriminative power for exclusion of germline SNVs by considering mutual overlaps

We estimated the discriminative power for the exclusion of germline SNVs by considering those from other non-cancerous exomes. Germline SNVs from 97 paired tumor-normal exomes were used as reference datasets. Up to 217 samples (96 normal tissue exomes from others and 121 additional Japanese exomes) were randomly selected, and their sensitivities and specificities for detecting the germline SNVs were detected by taking the averages of either all of the combinations or a subset of approximately 10,000 combinations. We also estimated the discriminative power with

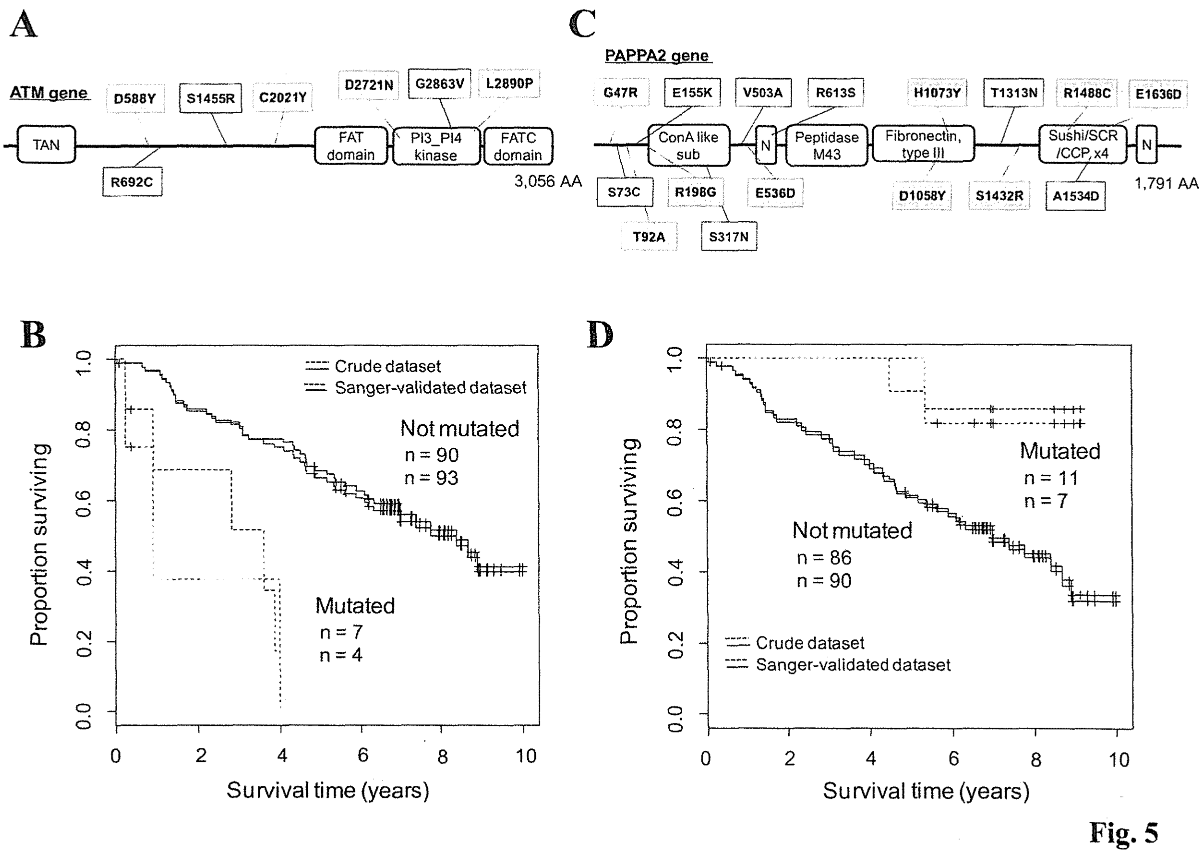

Fig. 5

Figure 5. Identification of the putative prognosis-related genes. (**A**) SNVs in the ATM gene. The SNVs that were identified in the initial screening and those remaining after the Sanger sequencing validation of the normal-tissue counterpart were shown in black and red, respectively. TAN: Telomere-length maintenance and DNA damage repair; PI3_PI4 kinase: Phosphatidylinositol 3-/4-kinase, catalytic. (**B**) Survival analysis of patients with and without ATM SNVs. The datasets before and after the Sanger sequencing validation are represented by black and red lines, respectively. Statistical significance was calculated using a log-rank test ($P < 0.05$). Note that the survival differences for individuals with SNVs in the non-Sanger-validated dataset were significant before the Sanger validation. (**C, D**) Results of a similar analysis as that described in A and B for the PAPPA2 gene. In this case, the patients with the SNVs showed better prognoses. ConA like sub: Concanavalin A-like lectin/glucanase, subgroup; N: Notch dimain; Peptidase M43: Peptidase M43, pregnancy-associated plasma-A.

doi: 10.1371/journal.pone.0073484.g005

Table 3. Comparison of the results in the enrichment analyses between the crude and refined dataset.

	Number of identified genes/pathways		
	Crude*	**Refined†**	**Overlap‡**
Genes	16	11	9
Pathways	23	26	19

* Identified using the crude dataset.

† Identified using the refined dataset.

‡ Significant in both crude and refined datasets.

doi: 10.1371/journal.pone.0073484.t003

data from the 1000 Genomes Project for four ethnic groups (73 JPT, 90 CHS, 81 YRI and 64 CEU) using similar trials. Whole-exome sequences (the phase1 exome data, 20110521) were obtained from the ftp site in the 1000 Genomes Project.

Kaplan-Meier curves

The Kaplan-Meier method was used to test the relations of the observed mutations to survival time, and calculations were performed using the R software package. Changes in survival rates that were correlated with SNVs were examined using the log-rank test (R survdiff).

Data access

Full raw datasets will be shared with researchers upon request. The information of somatic mutations at the respective genomic coordinates has been provided in Table **S2**.

Supporting Information

File S1. Figures S1 to S12 and Tables S3 to S11 are included.
(PDF)

Table S1. The comparison of our dataset with the other different study. We provided the comparison of our dataset with the genes identified in the other different study with transcriptome and epigenome data in lung cancers.
(XLSX)

Table S2. The list of somatic mutations identified from the refined dataset. All mutations described in this table are somatic and non-synonymous mutations.
(XLSX)

Acknowledgements

We thank W. Makałowski for constructive comments and suggestions for this manuscript. We are also grateful to F. Todokoro and F. Iguchi for their technical assistance with the data processing and N. Ogasawara for the Sanger sequencing validation.

Author Contributions

Conceived and designed the experiments: KT YS HE KG SS. Performed the experiments: SM YY AK KM MS. Analyzed the data: AS YS KT. Contributed reagents/materials/analysis tools: KG KT. Wrote the manuscript: AS KT YS.

References

1. The 1000 Genomes Project Consortium (2010) A map of human genome variation from population-scale sequencing. Nature 467: 1061-1073. doi:10.1038/nature09534. PubMed: 20981092.
2. The 1000 Genomes Project Consortium (2012) An integrated map of genetic variation from 1,092 human genomes. Nature 491: 56-65. doi: 10.1038/nature11632. PubMed: 23128226.
3. Choi M, Scholl UI, Ji W, Liu T, Tikhonova IR et al. (2009) Genetic diagnosis by whole exome capture and massively parallel DNA sequencing. Proc Natl Acad Sci U S A 106: 19096-19101. doi:10.1073/pnas.0910672106. PubMed: 19861545.
4. Ng SB, Turner EH, Robertson PD, Flygare SD, Bigham AW et al. (2009) Targeted capture and massively parallel sequencing of 12 human exomes. Nature 461: 272-276. doi:10.1038/nature08250. PubMed: 19684571.
5. Clark MJ, Chen R, Lam HY, Karczewski KJ, Chen R et al. (2011) Performance comparison of exome DNA sequencing technologies. Nat Biotechnol 29: 908-914. doi:10.1038/nbt.1975. PubMed: 21947028.
6. Bamshad MJ, Ng SB, Bigham AW, Tabor HK, Emond MJ et al. (2011) Exome sequencing as a tool for Mendelian disease gene discovery. Nat Rev Genet 12: 745-755. doi:10.1038/nrg3031. PubMed: 21946919.
7. Ng SB, Buckingham KJ, Lee C, Bigham AW, Tabor HK et al. (2010) Exome sequencing identifies the cause of a mendelian disorder. Nat Genet 42: 30-35. doi:10.1038/ng.499. PubMed: 19915526.
8. Biesecker LG (2010) Exome sequencing makes medical genomics a reality. Nat Genet 42: 13-14. doi:10.1038/ng0110-13. PubMed: 20037612.
9. Louis-Dit-Picard H, Barc J, Trujillano D, Miserey-Lenkei S, Bouatia-Naji N et al. (2012) KLHL3 mutations cause familial hyperkalemic hypertension by impairing ion transport in the distal nephron. Nat Genet.
10. Sherry ST, Ward MH, Kholodov M, Baker J, Phan L et al. (2001) dbSNP: the NCBI database of genetic variation. Nucleic Acids Res 29: 308-311. doi:10.1093/nar/29.1.308. PubMed: 11125122.
11. Futreal PA, Coin L, Marshall M, Down T, Hubbard T et al. (2004) A census of human cancer genes. Nat Rev Cancer 4: 177-183. doi: 10.1038/nrc1299. PubMed: 14993899.
12. International Cancer Genome Consortium (2010) International network of cancer genome projects. Nature 464: 993-998. doi:10.1038/nature08987. PubMed: 20393554.
13. Totoki Y, Tatsuno K, Yamamoto S, Arai Y, Hosoda F et al. (2011) High-resolution characterization of a hepatocellular carcinoma genome. Nat Genet 43: 464-469. doi:10.1038/ng.804. PubMed: 21499249.
14. Jones DT, Jäger N, Kool M, Zichner T, Hutter B et al. (2012) Dissecting the genomic complexity underlying medulloblastoma. Nature 488: 100-105. doi:10.1038/nature11284. PubMed: 22832583.
15. The Cancer Genome Atlas Research Network (2011) Integrated genomic analyses of ovarian carcinoma. Nature 474: 609-615. doi: 10.1038/nature10166. PubMed: 21720365.
16. Stephens PJ, Tarpey PS, Davies H, Van Loo P, Greenman C et al. (2012) The landscape of cancer genes and mutational processes in breast cancer. Nature 486: 400-404. PubMed: 22722201.
17. The Cancer Genome Atlas Research Network (2012) Comprehensive genomic characterization of squamous cell lung cancers. Nature.
18. The Cancer Genome Atlas Research Network (2012) Comprehensive molecular characterization of human colon and rectal cancer. Nature 487: 330-337. doi:10.1038/nature11252. PubMed: 22810696.
19. Imielinski M, Berger AH, Hammerman PS, Hernandez B, Pugh TJ et al. (2012) Mapping the hallmarks of lung adenocarcinoma with massively parallel sequencing. Cell 150: 1107-1120. doi:10.1016/j.cell.2012.08.029. PubMed: 22980975.
20. Davies H, Hunter C, Smith R, Stephens P, Greenman C et al. (2005) Somatic mutations of the protein kinase gene family in human lung cancer. Cancer Res 65: 7591-7595. PubMed: 16140923.
21. Ding L, Getz G, Wheeler DA, Mardis ER, McLellan MD et al. (2008) Somatic mutations affect key pathways in lung adenocarcinoma. Nature 455: 1069-1075. doi:10.1038/nature07423. PubMed: 18948947.
22. Kan Z, Jaiswal BS, Stinson J, Janakiraman V, Bhatt D et al. (2010) Diverse somatic mutation patterns and pathway alterations in human cancers. Nature 466: 869-873. doi:10.1038/nature09208. PubMed: 20668451.
23. Forbes SA, Bhamra G, Bamford S, Dawson E, Kok C et al. (2008) The Catalogue of Somatic Mutations in Cancer (COSMIC). Curr Protoc Hum Genet Chapter 10: Unit 10.11: PubMed: 18428421
24. Forbes SA, Bindal N, Bamford S, Cole C, Kok CY et al. (2011) COSMIC: mining complete cancer genomes in the Catalogue of Somatic Mutations in Cancer. Nucleic Acids Res 39: D945-D950. doi: 10.1093/nar/gkq929. PubMed: 20952405.
25. Li H, Durbin R (2009) Fast and accurate short read alignment with Burrows-Wheeler transform. Bioinformatics 25: 1754-1760. doi: 10.1093/bioinformatics/btp324. PubMed: 19451168.
26. McKenna A, Hanna M, Banks E, Sivachenko A, Cibulskis K et al. (2010) The Genome Analysis Toolkit: a MapReduce framework for analyzing next-generation DNA sequencing data. Genome Res 20: 1297-1303. doi:10.1101/gr.107524.110. PubMed: 20644199.
27. DePristo MA, Banks E, Poplin R, Garimella KV, Maguire JR et al. (2011) A framework for variation discovery and genotyping using next-generation DNA sequencing data. Nat Genet 43: 491-498. doi: 10.1038/ng.806. PubMed: 21478889.
28. Welch HC, Coadwell WJ, Ellson CD, Ferguson GJ, Andrews SR et al. (2002) P-Rex1, a PtdIns(3,4,5)P3- and Gbetagamma-regulated guanine-nucleotide exchange factor for Rac. Cell 108: 809-821. doi: 10.1016/S0092-8674(02)00663-3. PubMed: 11955434.

29. Rosenfeldt H, Vázquez-Prado J, Gutkind JS (2004) P-REX2, a novel PI-3-kinase sensitive Rac exchange factor. FEBS Lett 572: 167-171. doi:10.1016/j.febslet.2004.06.097. PubMed: 15304342.
30. Das B, Shu X, Day GJ, Han J, Krishna UM et al. (2000) Control of intramolecular interactions between the pleckstrin homology and Dbl homology domains of Vav and Sos1 regulates Rac binding. J Biol Chem 275: 15074-15081. doi:10.1074/jbc.M907269199. PubMed: 10748082.
31. Hill K, Krugmann S, Andrews SR, Coadwell WJ, Finan P et al. (2005) Regulation of P-Rex1 by phosphatidylinositol (3,4,5)-trisphosphate and Gbetagamma subunits. J Biol Chem 280: 4166-4173. PubMed: 15545267.
32. Chhatriwala MK, Betts L, Worthylake DK, Sondek J (2007) The DH and PH domains of Trio coordinately engage Rho GTPases for their efficient activation. J Mol Biol 368: 1307-1320. doi:10.1016/j.jmb.2007.02.060. PubMed: 17391702.
33. Sosa MS, Lopez-Haber C, Yang C, Wang H, Lemmon MA et al. (2010) Identification of the Rac-GEF P-Rex1 as an essential mediator of ErbB signaling in breast cancer. Mol Cell 40: 877-892. doi:10.1016/j.molcel.2010.11.029. PubMed: 21172654.
34. Kanehisa M, Goto S, Furumichi M, Tanabe M, Hirakawa M (2010) KEGG for representation and analysis of molecular networks involving diseases and drugs. Nucleic Acids Res 38: D355-D360. doi:10.1093/nar/gkp896. PubMed: 19880382.
35. Hecht JL, Mutter GL (2006) Molecular and pathologic aspects of endometrial carcinogenesis. J Clin Oncol 24: 4783-4791. doi:10.1200/JCO.2006.06.7173. PubMed: 17028294.
36. Li C, Fang R, Sun Y, Han X, Li F et al. (2011) Spectrum of oncogenic driver mutations in lung adenocarcinomas from East Asian never smokers. PLOS ONE 6: e28204. doi:10.1371/journal.pone.0028204. PubMed: 22140546.
37. Shigematsu H, Lin L, Takahashi T, Nomura M, Suzuki M et al. (2005) Clinical and biological features associated with epidermal growth factor receptor gene mutations in lung cancers. J Natl Cancer Inst 97: 339-346. doi:10.1093/jnci/dji055. PubMed: 15741570.
38. Sharma SV, Bell DW, Settleman J, Haber DA (2007) Epidermal growth factor receptor mutations in lung cancer. Nat Rev Cancer 7: 169-181. doi:10.1038/nrc2088. PubMed: 17318210.
39. Bos JL (1989) ras oncogenes in human cancer: a review. Cancer Res 49: 4682-4689. PubMed: 2547513.
40. Degen M, Brellier F, Kain R, Ruiz C, Terracciano L et al. (2007) Tenascin-W is a novel marker for activated tumor stroma in low-grade human breast cancer and influences cell behavior. Cancer Res 67: 9169-9179. doi:10.1158/0008-5472.CAN-07-0666. PubMed: 17909022.
41. Degen M, Brellier F, Schenk S, Driscoll R, Zaman K et al. (2008) Tenascin-W, a new marker of cancer stroma, is elevated in sera of colon and breast cancer patients. Int J Cancer 122: 2454-2461. doi:10.1002/ijc.23417. PubMed: 18306355.
42. Brellier F, Martina E, Degen M, Heuzé-Vourc'h N, Petit A et al. (2012) Tenascin-W is a better cancer biomarker than tenascin-C for most human solid tumors. BMC Clin Pathol 12: 14. doi:10.1186/1472-6890-12-14. PubMed: 22947174.
43. Dasika GK, Lin SC, Zhao S, Sung P, Tomkinson A et al. (1999) DNA damage-induced cell cycle checkpoints and DNA strand break repair in development and tumorigenesis. Oncogene 18: 7883-7899. PubMed: 10630641.
44. Bartkova J, Horejsi Z, Koed K, Kramer A, Tort F et al. (2005) DNA damage response as a candidate anti-cancer barrier in early human tumorigenesis. Nature 434: 864-870. doi:10.1038/nature03482. PubMed: 15829956.
45. Yan X, Baxter RC, Firth SM (2010) Involvement of pregnancy-associated plasma protein-A2 in insulin-like growth factor (IGF) binding protein-5 proteolysis during pregnancy: a potential mechanism for increasing IGF bioavailability. J Clin Endocrinol Metab 95: 1412-1420. doi:10.1210/jc.2009-2277. PubMed: 20103653.
46. Overgaard MT, Boldt HB, Laursen LS, Sottrup-Jensen L, Conover CA et al. (2001) Pregnancy-associated plasma protein-A2 (PAPP-A2), a novel insulin-like growth factor-binding protein-5 proteinase. J Biol Chem 276: 21849-21853. doi:10.1074/jbc.M102191200. PubMed: 11264294.
47. Shimasaki S, Shimonaka M, Zhang HP, Ling N (1991) Identification of five different insulin-like growth factor binding proteins (IGFBPs) from adult rat serum and molecular cloning of a novel IGFBP-5 in rat and human. J Biol Chem 266: 10646-10653. PubMed: 1709938.
48. Su Y, Wagner ER, Luo Q, Huang J, Chen L et al. (2011) Insulin-like growth factor binding protein 5 suppresses tumor growth and metastasis of human osteosarcoma. Oncogene 30: 3907-3917. doi:10.1038/onc.2011.97. PubMed: 21460855.
49. Huang T, Jiang M, Kong X, Cai YD (2012) Dysfunctions associated with methylation, microRNA expression and gene expression in lung cancer. PLOS ONE 7: e43441. doi:10.1371/journal.pone.0043441. PubMed: 22912875.
50. Li H, Handsaker B, Wysoker A, Fennell T, Ruan J et al. (2009) The Sequence Alignment/Map format and SAMtools. Bioinformatics 25: 2078-2079. doi:10.1093/bioinformatics/btp352. PubMed: 19505943.
51. Fujimoto A, Nakagawa H, Hosono N, Nakano K, Abe T et al. (2010) Whole-genome sequencing and comprehensive variant analysis of a Japanese individual using massively parallel sequencing. Nat Genet 42: 931-936. doi:10.1038/ng.691. PubMed: 20972442.
52. Quevillon E, Silventoinen V, Pillai S, Harte N, Mulder N et al. (2005) InterProScan: protein domains identifier. Nucleic Acids Res 33: W116-W120. doi:10.1093/nar/gni118. PubMed: 15980438.

Cancer Science
The official journal of the Japanese Cancer Association
JCA

Identification of a lung adenocarcinoma cell line with CCDC6-RET fusion gene and the effect of RET inhibitors *in vitro* and *in vivo*

Makito Suzuki,[1,2,11] Hideki Makinoshima,[1,11] Shingo Matsumoto,[1,3] Ayako Suzuki,[4] Sachiyo Mimaki,[1] Koutatsu Matsushima,[1,2] Kiyotaka Yoh,[3] Koichi Goto,[3] Yutaka Suzuki,[4] Genichiro Ishii,[5] Atsushi Ochiai,[5] Koji Tsuta,[6] Tatsuhiro Shibata,[7] Takashi Kohno,[8] Hiroyasu Esumi[9] and Katsuya Tsuchihara[1,2,10]

[1]Division of Translational Research, Research Center for Innovative Oncology, National Cancer Center Hospital East, Kashiwa, Chiba; [2]Department of Integrated Biosciences, Graduate School of Frontier Sciences, The University of Tokyo, Kashiwa, Chiba; [3]Division of Thoracic Oncology, National Cancer Center Hospital East, Kashiwa, Chiba; [4]Department of Medical Genome Sciences, Graduate School of Frontier Sciences, The University of Tokyo, Kashiwa, Chiba; [5]Division of Pathology, Research Center for Innovative Oncology, National Cancer Center Hospital East, Kashiwa, Chiba; [6]Division of Pathology and Clinical Laboratories, National Cancer Center Hospital, Tokyo; Divisions of [7]Cancer Genomics; [8]Genome Biology, National Cancer Center Research Institute, Tokyo; [9]National Cancer Center Hospital East, Kashiwa, Chiba, Japan

(Received December 4, 2012/Revised April 1, 2013/Accepted April 1, 2013/Accepted manuscript online April 11, 2013/Article first published online May 12, 2013)

Rearrangements of the proto-oncogene *RET* are newly identified potential driver mutations in lung adenocarcinoma (LAD). However, the absence of cell lines harboring *RET* fusion genes has hampered the investigation of the biological relevance of RET and the development of RET-targeted therapy. Thus, we aimed to identify a *RET* fusion positive LAD cell line. Eleven LAD cell lines were screened for *RET* fusion transcripts by reverse transcription-polymerase chain reaction. The biological relevance of the *CCDC6-RET* gene products was assessed by cell growth, survival and phosphorylation of ERK1/2 and AKT with or without the suppression of RET expression using RNA interference. The efficacy of RET inhibitors was evaluated *in vitro* using a culture system and in an *in vivo* xenograft model. Expression of the *CCDC6-RET* fusion gene in LC-2/ad cells was demonstrated by the mRNA and protein levels, and the genomic break-point was confirmed by genomic DNA sequencing. Mutations in *KRAS* and *EGFR* were not observed in the LC-2/ad cells. CCDC6-RET was constitutively active, and the introduction of a siRNA targeting the *RET 3'* region decreased cell proliferation by downregulating RET and ERK1/2 phosphorylation. Moreover, treatment with RET-inhibitors, including vandetanib, reduced cell viability, which was accompanied by the downregulation of the AKT and ERK1/2 signaling pathways. Vandetanib exhibited anti-tumor effects in the xenograft model. Endogenously expressing CCDC6-RET contributed to cell growth. The inhibition of kinase activity could be an effective treatment strategy for LAD. LC-2/ad is a useful model for developing fusion RET-targeted therapy. (*Cancer Sci* 2013; 104: 896–903)

Lung cancer is the most common cause of cancer death worldwide.(1) The identification of oncogenic driver genes is to select the increasing number of small molecule inhibitors targeting these gene products.(2,3) In particular, in lung adenocarcinoma (LAD), the most dominant histological subtype of lung cancer, the application of kinase inhibitors for cases with specific gene alterations has been successful, that is, gefitinib and erlotinib for *EGFR* mutation-positive cases and crizotinib for *ALK* fusion-positive cases.(4–7) Furthermore, accumulating evidence has demonstrated somatic mutations and rearrangements of potential oncogenes, including *BRAF, ERBB2* and *ROS1*, in LAD.(8–10)

RET is one of the newest LAD driver genes.(11–15) *RET* gene is located on chromosome 10 and encodes a receptor tyrosine kinase,(16,17) and the oncogenic potential of this gene product has been suggested in several tumors, including thyroid cancer.(18–20) Recently, five independent groups identified aberrant fusion genes, *KIF5B-RET* and *CCDC6-RET* in clinical samples of LAD.(11–15) Ectopically expressed RET fusion products afforded NIH3T3 cells with anchorage-independent growth and tumorigenicity in nude mice.(11,14) Furthermore, KIF5B-RET-expressing H1299 cells exhibited growth factor-independent growth.(11) These findings strongly suggest the oncogenic activity of RET fusion products and also suggest the potential therapeutic efficacy of multi-kinase inhibitor targeting of RET using the abovementioned cells. However, LAD-derived cell lines harboring *RET* fusion genes had not been identified. Recently, Matsubara *et al.*(21) screened LAD cell lines that were sensitive to a RET inhibitor vandetanib and found a *CCDC6-RET* fusion gene-harboring cell line, LC-2/ad.

We have independently screened cell lines established from Japanese LAD samples by RT-PCR and found that LC-2/ad cells expressed the *CCDC6-RET* fusion gene product. We further examined whether LC-2/ad cells depend on RET fusion-mediated signaling. In addition, the antitumor effect of RET inhibitors in LC-2/ad cells was evaluated *in vitro* and *in vivo*.

Materials and Methods

Complete materials and methods were described in the supplementary information (Data S1. Materials and Methods).

Purchased materials. Cell lines were purchased from RIKEN Bio Resource Center, the Immuno-Biological Laboratories (Fujioka, Japan) and American Type Culture Collection. Procedures for western blotting was previously described.(22) Primary antibodies specific for RET and phospho-RET Tyr-905 were purchased from Epitomics (Burlingame, CA, USA) and Cell Signaling Technologies (Danvers, MA, USA), respectively. RET-targeting siRNA was purchased from Life Technologies (Carlsbad, CA, USA). Gefitinib, sunitinib malate and sorafenib were purchased from Santa Cruz Biotechnology (Dallas, TX, USA), Sigma-Aldrich (St. Louis, MO, USA) and Toronto Research Chemicals (Toronto, ON, Canada),

[10]To whom correspondence should be addressed.
E-mail: ktsuchih@east.ncc.go.jp
[11]These authors contributed equally to this work.

doi: 10.1111/cas.12175
© 2013 Japanese Cancer Association

respectively. Vandetanib, AZD6244 and BEZ235 were purchased from Selleck (Houston, TX, USA).

Multiplex RT-PCR. Reported *KIF5B/CCDC6-RET* fusion variants were detected by multiplex RT-PCR according to the procedures described elsewhere.[11,14]

Genomic DNA sequencing. LC-2/ad DNA was captured with custom hybridization probes targeting *CCDC6* intron 1 and *RET* whole gene (Agilent) followed by parallel sequencing on the MiSeq system (Illumina).

Real-time RT-PCR. Procedures for real-time RT-PCR was previously described.[22] The PCR primers used in the present study are shown in Table S1.

***In vivo* studies.** LC2/ad cells at 5.0×10^6 were subcutaneously inoculated to 8-week-old athymic nude mice (Clea Japan).[23] Vandetanib was administered once daily as a homogeneous suspension by oral gavage at a dosage of 50 mg/kg body weight.[24] The tumor volume was calculated as the product of a scaling factor ($\pi/6$) and the tumor length, width and height.[22] The study was approved by the Institutional Ethics Review Committee for animal experiments at the National Cancer Center.

Immunohistochemical analysis. The procedure for hematoxylin eosin staining and immunohistochemical (IHC) was previously described.[22,25]

Microarray analysis. Background information of clinical samples was described in a previous report.[26] The study was approved by the Institutional Review Boards of the National Cancer Center. Total RNA was analyzed using Affymetrix (Santa Clara, CA, USA) U133Plus2.0 arrays. The data were processed by the MAS5 algorithm, and the mean expression level of a total of 54 675 probes was adjusted to 1000 for each sample.

Results

Identification of the *CCDC6-RET* fusion gene in a Japanese LAD cell line. To identify *RET* fusion-derived mRNA expression in human LAD cell lines, all reported *KIF5B-RET* and *CCDC6-RET* gene products were screened by multiplex RT-PCR in 11 cell lines derived from Japanese patients. LC-2/ad cells were found to express *CCDC6-RET* mRNA at significantly higher levels, whereas the other cell lines did not exhibit any fusion gene products (Fig. 1a). The expressed fusion *RET* product was sequenced, and an in-frame fusion of *CCDC6* exon 1 and *RET* exon 12, which was identical to the previously reported *CCDC6-RET* fusion products, was identified (Fig. 1b).[14] We then identified a breakpoint of chromosome 10 by retrieving genomic DNA fragments, including the entire *RET* gene and intron 1 of *CCDC6*, by target capture system followed by parallel sequencing. The identified break-point between *CCDC6* intron 1 and *RET* exon 11 was confirmed by Sanger sequencing (Fig. 1b). Quantitative RT-PCR revealed that the expression of 3′ end of *RET* was increased comparable to that of *CCDC6*, whereas the transcript level of the 5′ end of *RET* was significantly lower (Fig. 1c). Consistent with the amount of transcript, western blotting using an antibody recognizing the C-terminus of RET isoform 2 detected a 60-kDa specific band equivalent to

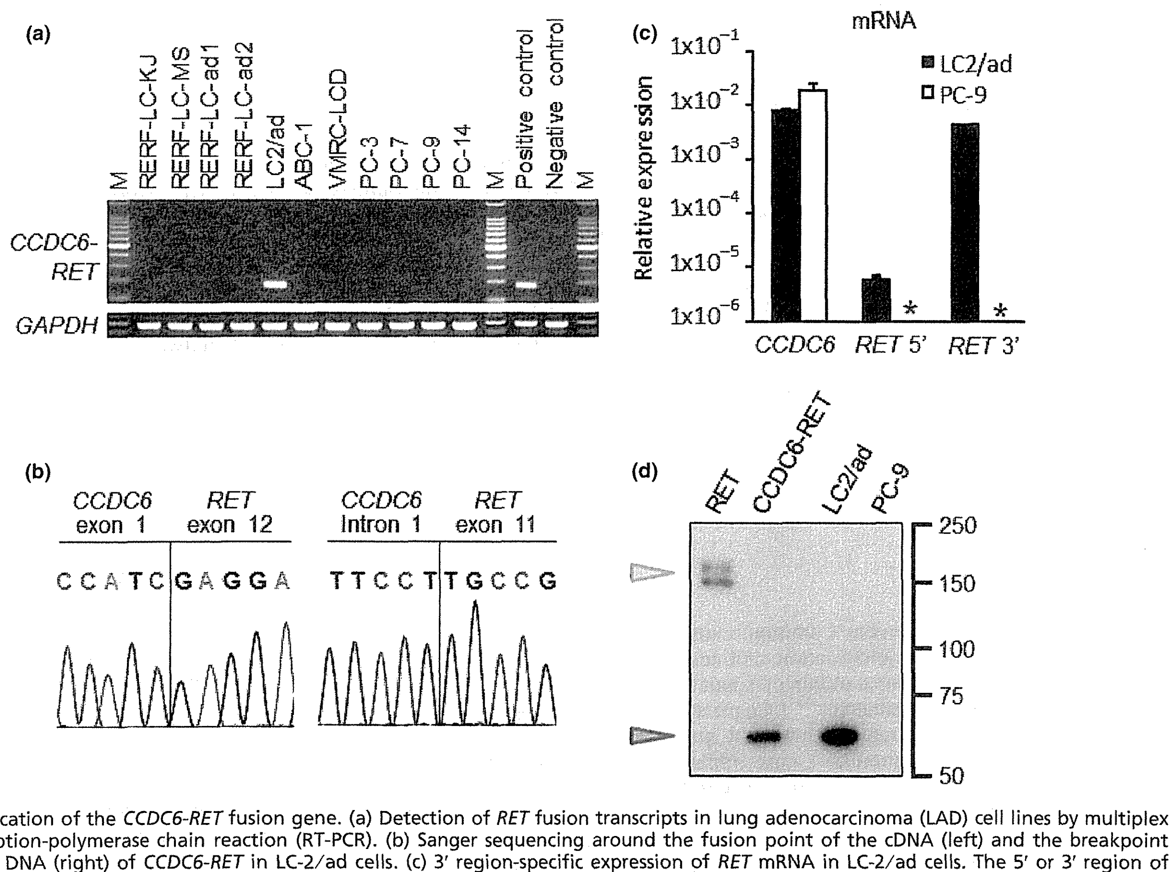

Fig. 1. Identification of the *CCDC6-RET* fusion gene. (a) Detection of *RET* fusion transcripts in lung adenocarcinoma (LAD) cell lines by multiplex reverse transcription-polymerase chain reaction (RT-PCR). (b) Sanger sequencing around the fusion point of the cDNA (left) and the breakpoint of the genomic DNA (right) of *CCDC6-RET* in LC-2/ad cells. (c) 3′ region-specific expression of *RET* mRNA in LC-2/ad cells. The 5′ or 3′ region of *RET* and *CCDC6* cDNA level was normalized to glyceraldehyde 3-phosphate dehydrogenase (*GAPDH*) expression. The data are shown as the mean ± standard deviation (SD) (n = 3). Asterisks indicate that mRNA expression were below the level of detection. (d) Specific expression of the CCDC6-RET fusion protein. Whole-cell lysates of LC2/ad and PC-9 cells and HEK293 cells transfected with wild-type RET (RET) or CCDC6-RET expression plasmids were subjected to western blot analysis to detect RET protein isoform 2. The LC-2/ad cells showed an approximately 60-kDa (red arrowhead) but not 170-kDa (blue arrowhead) band.

© 2013 Japanese Cancer Association

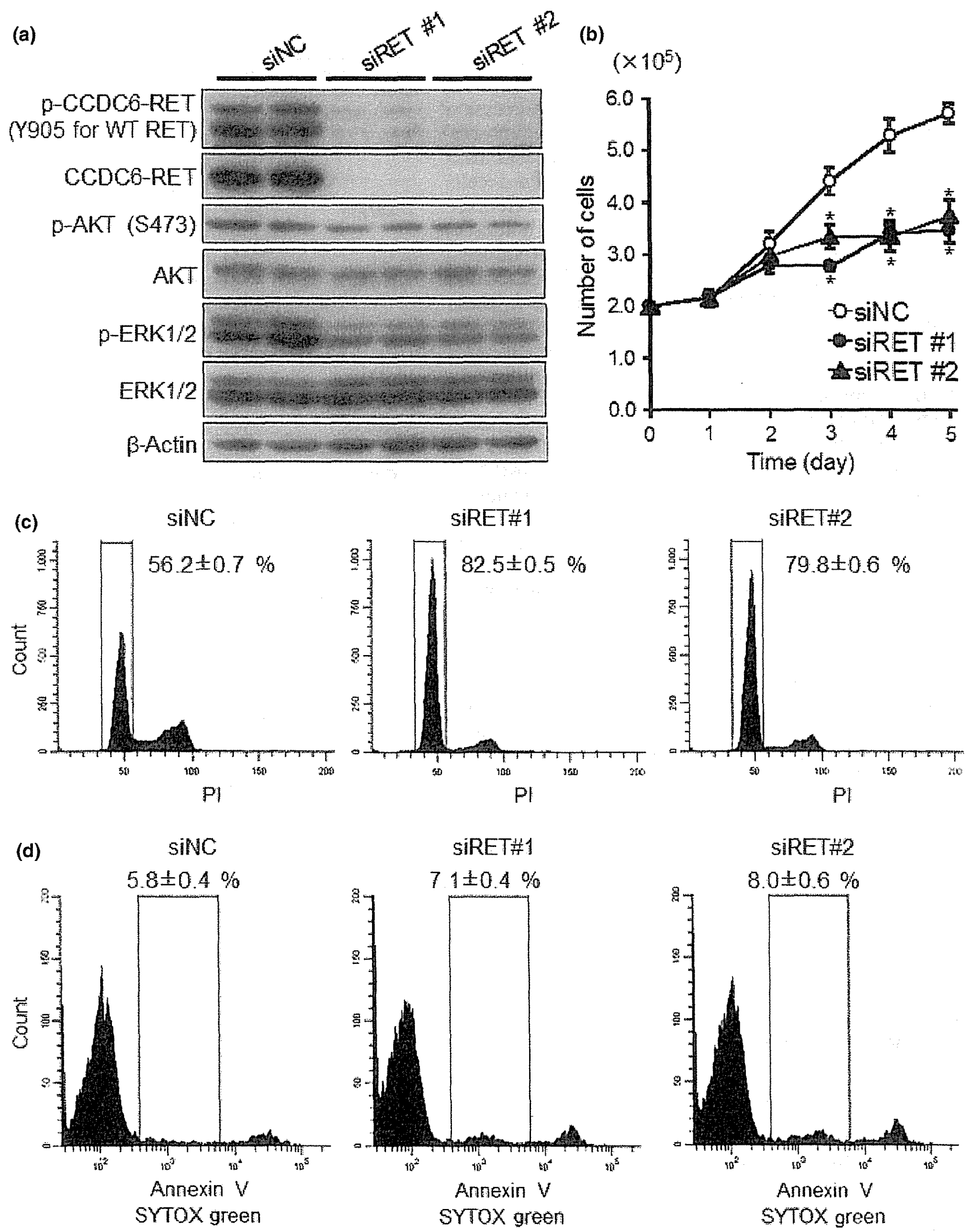

Fig. 2. Suppression of CCDC-RET expression by siRNA in LC-2/ad cells. (a) Western blot analysis of siRET-treated LC-2/ad cells. The siRNA transfected cell lysates were applied to the western blotting. (b) Involvement of RET suppression in cell growth inhibition. LC-2/ad cells transfected with siRNAs were incubated for the indicated times. The data are shown as the mean ± standard deviation (SD) ($n = 4$). *$P < 0.01$ (Student's *t*-test). (c,d) The DNA ploidy (c) and Annexin V-positive population (d) of siRET-transfected LC-2/ad cells. After 72 h of siRNA transfection, the cells were subjected to DNA ploidy analysis and Annexin V staining. The data are shown as the mean ± SD ($n = 4$).

the estimated size of the fusion protein composed of 503 amino acids (GeneBank BAM36435), whereas no significant signal was detected that approximated the size of wild-type RET, 170-kDa (Fig. 1d).[11] Taken together, we concluded that LC-2/ad cells express *CCDC6-RET* fusion gene products. *KRAS* exon 2 and *EGFR* exon 19 and 21 were examined by Sanger sequencing, but no obvious mutation was confirmed (Fig. S1).

CCDC6-RET-dependent ERK1/2 phosphorylation and the proliferation of LC-2/ad cells. We suppressed *RET* expression by RNAi to characterize the function of CCDC6-RET in LC-2/ad cells. For avoiding off-target siRNA effects, two different sequences of siRNA directed against the 3′ region of *RET* (siRET#1 and #2) and a nontargeting siRNA (siNC) were used. When compared to siNC, a significant reduction in mRNA expression was observed by quantitative RT-PCR detecting the 3′ end of the *RET* mRNA: 66.5% for siRET#1 and 94.2% for siRET#2 (Fig. S2). Western blot analyses also revealed significant decreases in the expression of CCDC6-RET protein (60-kDa) upon the introduction of siRET#1 and #2 compared to the control siNC in the LC-2/ad cells

doi: 10.1111/cas.12175
© 2013 Japanese Cancer Association

(Fig. 2a). To examine whether the downstream signaling pathway was altered by the introduction of siRNA, the phosphorylation of ERK1/2 and AKT was examined. The phospho-ERK1/2 signal was significantly decreased by the suppression of CCDC6-RET expression, whereas the decrease of AKT phosphorylation was marginal (Fig. 2a). The involvement of RET fusion in LC-2/ad cell proliferation was then examined. The number of live CCDC6-RET-suppressed cells decreased throughout the experiment, and the difference became significant at day 3 and thereafter (Fig. 2b). To address the growth suppression further, the cell cycle of the siRNA-treated cells were assessed by the DNA ploidy pattern. The LC-2/ad cells treated with siRET exhibited significant increases in the percent of cells arrested in the G1 phase relative to the cells treated with siNC (Fig. 2c). However, the apoptotic cells, as assessed by Annexin V positivity, was not significantly increased by the suppression of RET expression (Fig. 2d).

RET-dependent transcriptome profile in LC-2/ad cell. To characterize the transcriptome profile, which is regulated by CCDC6-RET and its downstream signaling pathway, siRET#2 and siNC treated LC-2/ad cells were subjected to genome-wide expression profiling using Affymetrix U133Plus2.0 arrays. A total of 243 genes, evaluated with 285 probes were selected as those preferentially suppressed by less than half in siRET-treated cells.As well, 566 genes with 661 probes were expressed more than twice in siRET-treated cells (Table S2 and Fig. S3). The *RET* gene itself (probe ID = 211421_s_at) showed the highest fold-difference of 19.6 between siNC- and siRET#2-treated cells. Following *RET*, previously identified Gene Ontology-annotated Ras-MAPK downstream genes like *DUSP6* was preferentially suppressed in the siRET-treated cells. In addition, cell cycle regulation-related genes like *EREG, CDC6, MCM10, MAD2L1, CHEK1* and *PLK4* were expressed <0.5-fold in siRET-treated cells (Table 1).

RET fusion gene screening of 300 consecutive surgically resected LAD samples identified one case of *CCDC6-RET* expressing LAD by RT-PCR and break-apart FISH (Tsuta *et al.*, 2012, unpublished data). We checked the expression level of potential CCDC6-RET-driven genes identified above in the clinical sample. Among 285 preferentially expressed probes, 81 probes were also upregulated more than twofold in the *CCDC6-RET* positive LAD tissue compared to the surrounding non-cancerous tissue (Table 1 and Table S2).

RET inhibitor-induced cell cycle arrest and apoptosis in LC-2/ad cells. The phosphorylation status of the tyrosine 905 residue of RET isoforms 2 and 4 was high in the LC-2/ad cells, regardless of the presence or absence of serum in the culture medium, whereas the total amount of RET isoform 2 was not significantly altered. Similarly, the phosphorylation status of AKT and ERK1/2 was high under serum-starved conditions, and the enhanced phosphorylation of these molecules was slight with serum stimulation, suggesting that the fusion RET kinase was constitutively active and activated its downstream signaling pathways (Fig. 3a).

Next, the effects of kinase inhibitors, which inhibit spectrum including RET were applied to evaluate their effects on the signaling pathways in the LC-2/ad cells. We treated the cells with RET inhibitors vandetanib, sunitinib and sorafenib at a final concentration of 10 μM, which was 10–30 times higher than the *in vitro* half maximal inhibitory concentration (IC_{50}) for RET kinase activity of each compound. Gefitinib, another small molecule inhibitor targeting EGFR but not RET,[13] was also examined. All the inhibitors except gefitinib significantly suppressed the phosphorylation of RET, AKT and ERK1/2. Although vandetanib, sunitinib and sorafenib equivalently suppressed RET phosphorylation, vandetanib most significantly suppressed the phosphorylation of ERK1/2 (Fig. 3a). The inhibitory effect of vandetanib on RET, AKT and ERK1/2

Table 1. Up- or downregulated genes associated with mitogen-activated protein kinase (MAPK) cascade or cell cycle

Gene symbol	Probe set ID	siNC/siRET	Tumor/Non-tumor
Upregulated			
RET	211421_s_at	19.63	19.52
	205879_x_at	3.76	5.03
	215771_x_at	2.37	4.72
DUSP6	208892_s_at	4.45	5.22
	208893_s_at	4.17	6.34
	208891_at	4.17	3.56
EREG	1569583_at	3.68	1.60
	205767_at	2.93	5.69
CDC6	203967_at	2.42	4.82
	203968_s_at	1.95	5.32
MCM10	220651_s_at	2.30	4.83
	223570_at	1.72	1.71
MAD2L1	203362_s_at	2.28	5.91
	1554768_a_at	1.91	4.34
CHEK1	205394_at	2.17	9.03
	205393_s_at	2.14	6.87
PLK4	204886_at	2.07	4.38
	204887_s_at	1.56	4.08
Downregulated			
MEF2C	209200_at	0.21	0.46
	209199_s_at	0.26	0.65
GAB1	214987_at	0.23	0.42
	229114_at	0.53	0.65
	225998_at	0.62	0.68
	226002_at	0.64	0.76
CDKN1C	216894_x_at	0.26	0.41
	213348_at	0.32	0.23
	213183_s_at	0.35	0.30
	219534_x_at	0.42	0.27
	213182_x_at	0.44	0.21
PTEN	233314_at	0.33	0.27
	225363_at	0.77	0.47
TIMP2	231579_s_at	0.34	0.33
	224560_at	0.37	0.27
ID2	201566_x_at	0.35	0.31
	201565_s_at	0.40	0.39
	213931_at	0.52	0.31
CCNL2	232274_at	0.35	0.42
	222999_s_at	0.79	0.52
RPS6KA2	212912_at	0.41	0.34
	204906_at	0.59	0.49

phosphorylation exhibited concentration dependency (Fig. 3b). Gefitinib significantly suppressed EGFR phosphorylation while total EGFR protein level was not altered. Meanwhile, gefitinib did not alter the phosphorylation status of AKT and ERK1/2 (Fig. 3a). Meanwhile, vandetanib suppressed EGFR as well as AKT and ERK1/2 in *EGFR*-mutant PC-9 cells (Fig. S4).

We further examined the effect of the above inhibitors on the growth of the LC-2/ad cells using the WST-8 assay. Consistent with the effects of the inhibitors on the RET signaling pathway, vandetanib suppressed cell growth most significantly (IC_{50} = 0.32 μM), followed by sunitinib and sorafenib, whereas gefitinib only exhibited an apparent suppression at its highest dose (Fig. 3c). However, the effects of these inhibitors on *KRAS*-mutant A549 cells were much lower (Fig. S5). Gefitinib and vandetanib, both of which inhibit EGFR, suppressed *EGFR*-mutant PC-9 cells, whereas sunitinib and sorafenib had less effect (Fig. S5). Evaluating the number of live cells by trypan blue staining under the treatment of several doses of

© 2013 Japanese Cancer Association

vandetanib suggested a dose-dependent suppression in the LC-2/ad cells. Furthermore, the number of cells treated with 0.5 and 1.0 μM vandetanib was apparently reduced to less than the starting amount, strongly suggesting that vandetanib induced both cell death and the suppression of cell proliferation (Fig. 3d). An assessment of the DNA ploidy revealed that vandetanib arrested the cell cycle in G1 phase in a dose-dependent manner (Fig. 3e), and an increased concentration of vandetanib induced an Annexin V-positive apoptotic cell population (Fig. 3f). The proapoptotic effect of vandetanib was confirmed by the detection of cleaved caspase-3 by western blotting (Fig. 3b). Meanwhile, 1.0 μM sunitinib and sorafenib induced cell cycle arrest but induction of apoptosis was marginal (Figs S6 and S7).

To further evaluate the contribution of Ras-ERK and AKT axes to cell survival, LC-2/ad cells were treated with MEK1/2 inhibitor AZD6244 or PI3K/mTOR inhibitor BEZ235. Cytotoxic effect of AKT-inhibiting BEZ235 was more than that of ERK-inhibiting AZD6244. However, both inhibitors did not completely reduce the cell survival even their maximal dose (Figs S8 and S9).

Anti-tumor effect of vandetanib in an LC-2/ad xenograft model. Subcutaneously transplanted LC-2/ad tumors exhibited typical adenocarcinoma morphology. These tumors were positive for SFTPA, Napsin A and carcinoembryonic antigen (CEA) but thyroid marker thyroglobulin negative using immunohistochemistry (IHC). Furthermore, using an antibody cross-reacting with both human and mouse RET protein, IHC revealed that RET was highly expressed specifically in the tumor cells but not in the interstitial cells (Fig. 4a). The over-expression of RET in these tumors was confirmed using quantitative RT-PCR and Western blotting. Similar to the results from cultured LC-2/ad cells, much more mRNA of the 3′ end of *RET* was detected than that of the 5′ end (Fig. 4b), and a specific band equivalent to the size of the CCDC6-RET fusion protein was detected (Fig. 4c). Vandetanib (50 mg/kg) was orally administrated to the mice harboring the LC-2/ad xenograft, and the daily administration of vandetanib significantly reduced the tumor size. Although the tumors were diminished at day 14 of the treatment, the body weight of the treated mice was not significantly reduced (Fig. 4d and Fig. S10). Sorafenib (30 mg/kg) and sunitinib (40 mg/kg) did not reduce the body weight, either (Fig. S10). Sorafenib reduced but not diminished the tumors at day14. Anti-tumor effect of sunitinib was not significant (Fig. S11).

Discussion

Previous reports suggest that the incidence of *RET*-fusion-positive cases in LAD is 1–2% and that these cases are concentrated in the *EGFR* mutation-, *KRAS* mutation-, and *ALK*-fusion-negative population.[10,27] To identify cell lines expressing endogenous *RET*-fusion genes, we selected 11 cell lines that were derived from pathologically identified Japanese LAD cases. Among them, activating EGFR mutations have been reported in PC-3 and PC-9 cells.[28] However, the mutation status of known driver genes of other cell lines was not well investigated. The LC-2/ad cells were originally derived from pleural effusion of LAD in a patient who had received combined chemotherapy (endoxan, Adriamycin, Cisplatin and mitomycin C)[23]; the cancer was diagnosed by cytological examination of the patient's sputum and pleural effusion. The original report indicated that the LC-2/ad cells were positive for an adenocarcinoma marker, cytokeratin 18.[23] In addition, we detected surfactant protein, an aspartate proteinase, Napsin A, and CEA expression in the xenograft tumor (Fig. 4a). These findings support the origin of LC-2/ad as lung adenocarcinoma. The modal chromosome number described in the original report was 53–56, though an apparent translocation between the chromosomes was not reported, consistent with the fact that the inversion of chromosome 10 was not obvious in the conventional chromosome counts.

The Sanger sequencing in this study and the whole-transcriptome sequencing (Tsuchihara, 2012, unpublished data) revealed no driver mutations of *KRAS*, *EGFR* and known genes other than the *CCDC6-RET* fusion in the LC-2/ad cells, highly suggesting that the CCDC6-RET fusion protein plays pivotal roles in the proliferation of these cells. The autophosphorylation of CCDC6-RET was clearly observed in a serum-independent manner, accompanied with a constitutive elevation of ERK1/2 phosphorylation. The suppression of CCDC6-RET expression induced a decrease in ERK1/2 phosphorylation, accompanied with a decrease in the expression of the genes that regulate the cell cycle. As a result, the CCDC6-RET-suppressed cells exhibited significant growth retardation.

Recently, a Japanese group independently reported the CCDC6-RET fusion in LC2/ad cells.[21] However, the efficacy of RET inhibitors to the RET and downstream pathways and *in vivo* anti-tumor effects have been partially described.[21] Vandetanib, sorafenib and sunitinib suppress the activities of multiple kinases, including RET, and have been approved for several cancers.[29–31] In *in vitro* analyses, these compounds effectively suppressed the phosphorylation of CCDC6-RET and suppressed proliferation and induced death in LC-2/ad cells. It should be noted that the IC_{50} value for the growth suppression of these compounds was equivalent to the dose suggested in a previous study using culture cells expressing ectopic *KIF5B-RET* cDNA.[13] These effects were most likely dependent on RET inhibition. Sunitinib and sorafenib did not affect PC-9 and A549 cells, which have activating mutations of *EGFR* and *KRAS*, respectively. Vandetanib presumably suppressed the growth of PC-9 cells, as EGFR is included in its inhibitory spectrum. Meanwhile, gefitinib, which targets EGFR but not RET, did not significantly suppress the growth of LC-2/ad cells. Interestingly, gefitinib did not alter the phosphorylation of AKT and ERK1/2 in LC-2/ad cells albeit equivalently suppressing EGFR phosphorylation as vandetanib. Although precise molecular mechanisms should be further examined, LC-2/ad cells might not depend on EGFR for transducing downstream signaling.

Vandetanib exhibited apparent anti-tumor effects in the xenograft model in this study. Recently, efficacy of vandetanib on thyroid cancer cells harboring *RET*-fusion gene was also reported.[32] These findings strongly suggest that RET inhibition is a plausible therapeutic strategy for RET-fusion-positive tumors.

We noticed a discrepancy between the effects of RNA interference and inhibitor treatment on RET. Though RET suppression/inhibition equivalently reduced the level of phosphorylated RET and induced cell cycle arrest, obvious apoptosis was not found in the cells treated with siRNA. A possible explanation is that CCDC6-RET is mainly involved in the RAS-ERK pathway to regulate cell proliferation, whereas the anti-apoptotic signaling pathway mediated by AKT could be regulated by other signaling molecules inhibited by the multi-kinase inhibitors. A recent study using a Drosophila *in vivo* screening system suggested that the antitumor effects and toxicity of RET inhibitors were dependent on the profile of the "off-target" inhibition of multiple kinases in addition to the specific inhibition of RET.[33] Further investigation elucidating the molecules and signaling pathways relevant to the cytotoxic effect of vandetanib in LC-2/ad cells is anticipated.

Whether LC-2/ad-based models adequately represent clinical *RET* fusion-positive LAD cases is another challenging question. Takeuchi stated that clinically identified *CCDC6-RET*-positive LAD exhibited a histologically cribriform pattern.[14]

doi: 10.1111/cas.12175
© 2013 Japanese Cancer Association

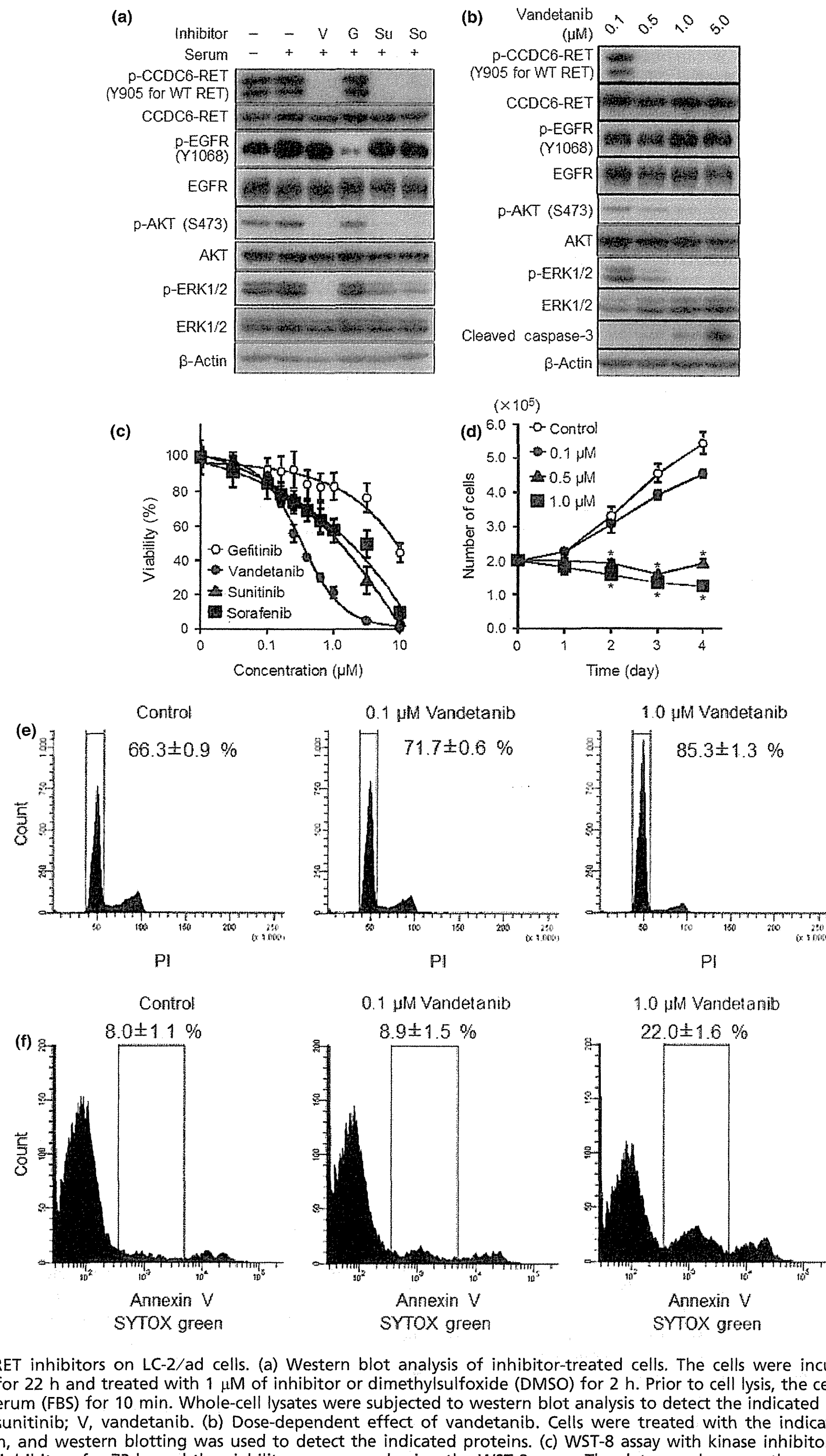

Fig. 3. Effect of RET inhibitors on LC-2/ad cells. (a) Western blot analysis of inhibitor-treated cells. The cells were incubated under serum-starved conditions for 22 h and treated with 1 μM of inhibitor or dimethylsulfoxide (DMSO) for 2 h. Prior to cell lysis, the cells were treated with 10% fetal bovine serum (FBS) for 10 min. Whole-cell lysates were subjected to western blot analysis to detect the indicated proteins. G, gefitinib; So, sorafenib; Su, sunitinib; V, vandetanib. (b) Dose-dependent effect of vandetanib. Cells were treated with the indicated concentration of vandetanib for 12 h, and western blotting was used to detect the indicated proteins. (c) WST-8 assay with kinase inhibitors. Cells were treated with the indicated inhibitors for 72 h, and the viability was assessed using the WST-8 assay. The data are shown as the mean ± standard deviation (SD) (n = 6). (d) Effect of vandetanib for growth inhibition. Cells were treated with vandetanib and incubated for the indicated time. The data are shown as the mean ± SD (n = 3). *P < 0.01 (Student's t test). (e,f) DNA ploidy (e) and Annexin V-positive population (f) of the cells treated with vandetanib for 48 h. The data are shown as the mean ± SD (n = 4).

© 2013 Japanese Cancer Association

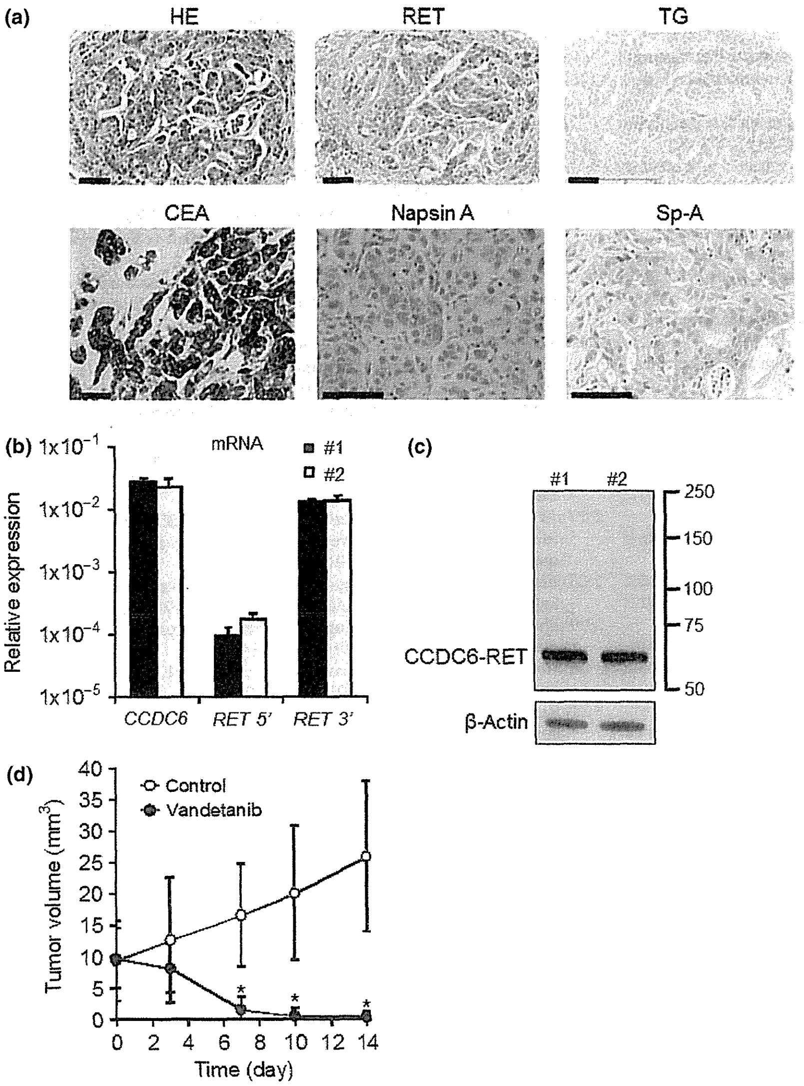

Fig. 4. Characterization of the LC-2/ad xenograft and anti-tumor effects of vandetanib. (a) Histological features of the xenograft. Hematoxylin and eosin staining and immunohistochemical staining with the indicated antibodies. Scale bars were 100 μm. Hematoxylin eosin (HE), RET, thyroglobulin (TG) and carcinoembryonic antigen (CEA) (×20); Napsin A and Sp-A (×40). (b) 3′ region-specific expression of *RET* mRNA in the xenograft. Total RNA extracted from tumors was subjected to real-time reverse transcription-polymerase chain reaction (RT-PCR) analysis with the primer sets designed for the 5′ or 3′ region of the *RET* and *CCDC6* cDNA. The data are shown as the mean ± standard deviation (SD) ($n = 3$). (c) Expression of the CCDC6-RET protein in mice xenografts. Whole-cell lysates of tumors were subjected to western blot analysis. (d) Anti-tumor effect of vandetanib *in vivo*. Vandetanib was administered once a day at a dosage of 50 mg/kg. The data are shown as the mean ± SD ($n = 9$). $^*P < 0.01$ (control *vs* sorafenib; Student's *t* test).

Because the cribriform structure was presumably developed from normal alveolar architecture, this specific morphology was not observed in the subcutaneously transplanted LC-2/ad tumors. We assume that the comparison of the transcriptome profile between the LC-2/ad cells and clinically identified LAD tissue samples may provide clues. Approximately one-third of the genes suppressed by RNA interference directed at *RET* overlapped with the genes preferentially expressed in the clinical tumor sample. Because we have had only one example of paired data, it is difficult to estimate the similarity between the cell line and clinical samples. However, the above overlap appears promising, and we will continue to screen both cell lines and clinical samples to accumulate comprehensive data.

In this study, the screening of Japanese LAD cell lines was effective for the identification of *RET* fusion-positive cancer cells, representing a clinically rare subpopulation. LC-2/ad cells might be useful in the development of RET-targeted therapies, that is, new compound screening, clarifying the pharmacological mechanisms and investigating the mechanisms for acquired resistance.

Acknowledgments

We thank Drs Hiroki Sasaki and Kazuhiko Aoyagi and the National Cancer Center Research Core Facility for the microarray analyses. The Core Facility was supported by National Cancer Center Research and Development Fund (23-A-7). This work was supported by National Cancer Center Research and Development Fund (23-A-8, 15, 24-A-1) and JSPS KAKENHI Grant number 24300345.

Disclosure Statement

The authors have no conflict of interest.

References

1 Jemal A, Bray F, Center MM, Ferlay J, Ward E, Forman D. Global cancer statistics. *CA Cancer J Clin* 2011; **61**: 69–90.

2 Pao W, Girard N. New driver mutations in non-small-cell lung cancer. *Lancet Oncol* 2011; **12**: 175–80.

3 Pao W, Chmielecki J. Rational, biologically based treatment of EGFR-mutant non-small-cell lung cancer. *Nat Rev Cancer* 2010; **10**: 760–74.

doi: 10.1111/cas.12175
© 2013 Japanese Cancer Association

4 Kwak EL, Bang YJ, Camidge DR *et al.* Anaplastic lymphoma kinase inhibition in non-small-cell lung cancer. *N Engl J Med* 2010; **363**: 1693–703.
5 Lynch TJ, Bell DW, Sordella R *et al.* Activating mutations in the epidermal growth factor receptor underlying responsiveness of non-small-cell lung cancer to gefitinib. *N Engl J Med* 2004; **350**: 2129–39.
6 Paez JG, Janne PA, Lee JC *et al.* EGFR mutations in lung cancer: correlation with clinical response to gefitinib therapy. *Science* 2004; **304**: 1497–500.
7 Tsao MS, Sakurada A, Cutz JC *et al.* Erlotinib in lung cancer – molecular and clinical predictors of outcome. *N Engl J Med* 2005; **353**: 133–44.
8 Govindan R, Ding L, Griffith M *et al.* Genomic landscape of non-small cell lung cancer in smokers and never-smokers. *Cell* 2012; **150**: 1121–34.
9 Imielinski M, Berger AH, Hammerman PS *et al.* Mapping the hallmarks of lung adenocarcinoma with massively parallel sequencing. *Cell* 2012; **150**: 1107–20.
10 Seo JS, Ju YS, Lee WC *et al.* The transcriptional landscape and mutational profile of lung adenocarcinoma. *Genome Res* 2012; **22**: 2109–19.
11 Kohno T, Ichikawa H, Totoki Y *et al.* KIF5B-RET fusions in lung adenocarcinoma. *Nat Med* 2012; **18**: 375–7.
12 Li F, Feng Y, Fang R *et al.* Identification of *RET* gene fusion by exon array analyses in "pan-negative" lung cancer from never smokers. *Cell Res* 2012; **22**: 928–31.
13 Lipson D, Capelletti M, Yelensky R *et al.* Identification of new *ALK* and *RET* gene fusions from colorectal and lung cancer biopsies. *Nat Med* 2012; **18**: 382–4.
14 Takeuchi K, Soda M, Togashi Y *et al.* RET, ROS1 and ALK fusions in lung cancer. *Nat Med* 2012; **18**: 378–81.
15 Wang R, Hu H, Pan Y *et al.* RET fusions define a unique molecular and clinicopathologic subtype of non-small-cell lung cancer. *J Clin Oncol* 2012; **30**: 4352–9.
16 Gardner E, Papi L, Easton DF *et al.* Genetic linkage studies map the multiple endocrine neoplasia type 2 loci to a small interval on chromosome 10q11.2. *Hum Mol Genet* 1993; **2**: 241–6.
17 Mole SE, Mulligan LM, Healey CS, Ponder BA, Tunnacliffe A. Localisation of the gene for multiple endocrine neoplasia type 2A to a 480 kb region in chromosome band 10q11.2. *Hum Mol Genet* 1993; **2**: 247–52.
18 Mulligan LM, Kwok JB, Healey CS *et al.* Germ-line mutations of the RET proto-oncogene in multiple endocrine neoplasia type 2A. *Nature* 1993; **363**: 458–60.
19 Hofstra RM, Landsvater RM, Ceccherini I *et al.* A mutation in the RET proto-oncogene associated with multiple endocrine neoplasia type 2B and sporadic medullary thyroid carcinoma. *Nature* 1994; **367**: 375–6.
20 Grieco M, Cerrato A, Santoro M, Fusco A, Melillo RM, Vecchio G. Cloning and characterization of H4 (D10S170), a gene involved in RET rearrangements *in vivo*. *Oncogene* 1994; **9**: 2531–5.
21 Matsubara D, Kanai Y, Ishikawa S *et al.* Identification of CCDC6-RET fusion in the human lung adenocarcinoma cell line, LC-2/ad. *J Thorac Oncol* 2012; **7**: 1872–6.
22 Makinoshima H, Ishii G, Kojima M *et al.* PTPRZ1 regulates calmodulin phosphorylation and tumor progression in small-cell lung carcinoma. *BMC Cancer* 2012; **12**: 537.
23 Kataoka H, Itoh H, Seguchi K, Koono M. Establishment and characterization of a human lung adenocarcinoma cell line (LC-2/ad) producing alpha 1-antitrypsin *in vitro*. *Acta Pathol Jpn* 1993; **43**: 566–73.
24 Wedge SR, Ogilvie DJ, Dukes M *et al.* ZD6474 inhibits vascular endothelial growth factor signaling, angiogenesis, and tumor growth following oral administration. *Cancer Res* 2002; **62**: 4645–55.
25 Yoshida A, Tsuta K, Nakamura H *et al.* Comprehensive histologic analysis of ALK-rearranged lung carcinomas. *Am J Surg Pathol* 2011; **35**: 1226–34.
26 Okayama H, Kohno T, Ishii Y *et al.* Identification of genes upregulated in ALK-positive and EGFR/KRAS/ALK-negative lung adenocarcinomas. *Cancer Res* 2012; **72**: 100–11.
27 Ju YS, Lee WC, Shin JY *et al.* A transforming *KIF5B* and *RET* gene fusion in lung adenocarcinoma revealed from whole-genome and transcriptome sequencing. *Genome Res* 2012; **22**: 436–45.
28 Blanco R, Iwakawa R, Tang M *et al.* A gene-alteration profile of human lung cancer cell lines. *Hum Mutat* 2009; **30**: 1199–206.
29 Phay JE, Shah MH. Targeting RET receptor tyrosine kinase activation in cancer. *Clin Cancer Res* 2010; **16**: 5936–41.
30 Antonelli A, Fallahi P, Ferrari SM *et al.* RET TKI: potential role in thyroid cancers. *Curr Oncol Rep* 2012; **14**: 97–104.
31 Scagliotti GV. Potential role of multi-targeted tyrosine kinase inhibitors in non-small-cell lung cancer. *Ann Oncol* 2007; **18**(Suppl 10): x32–41.
32 Couto JP, Almeida A, Daly L *et al.* AZD1480 blocks growth and tumorigenesis of RET- activated thyroid cancer cell lines. *PLoS ONE* 2012; **7**: e46869.
33 Dar AC, Das TK, Shokat KM, Cagan RL. Chemical genetic discovery of targets and anti-targets for cancer polypharmacology. *Nature* 2012; **486**: 80–4.

Supporting Information

Additional Supporting Information may be found in the online version of this article:

Data S1. Materials and methods.

Fig. S1. The absence of the known driver mutations.

Fig. S2. Suppression of *RET* mRNA in siRET-treated cells.

Fig. S3. RET-dependent transcriptome profile in LC-2/ad cells.

Fig. S4. Dose-dependent effect of vandetanib in PC-9 cells.

Fig. S5. WST-8 assay with various kinase inhibitors.

Fig. S6. Effect of sunitinib and sorafenib on G1 phase population of LC-2/ad cells.

Fig. S7. Effect of sunitinib and sorafenib on apoptosis of LC-2/ad cells.

Fig. S8. Dose-dependent effect of AZD6244 and BEZ235 in LC-2/ad cells.

Fig. S9. WST-8 assay of LC-2/ad cells treated with AZD6244 and BEZ235.

Fig. S10. Body weight of the vandetanib-, sunitinib-, sorafenib- and vehicle-treated mice.

Fig. S11. Effect of sunitinib and sorafenib *in vivo*.

Table S1. Polymerase chain reaction primers.

Table S2. Summary of the microarray data.

© 2013 Japanese Cancer Association